

---

## AN IMPROVED 2-PHASE SNAIL-CAM TYPE FAN MOTOR DESIGN

<sup>1</sup>Ji-Young Lee, <sup>1</sup>Geun-Ho Lee, <sup>1</sup>Jeong-Jong Lee,  
<sup>1</sup>Jung-Pyo Hong, *Senior Members, IEEE*, and <sup>2</sup>Kyung-Ho Ha

<sup>1</sup>Dept. of Electrical Eng., Changwon Nat'l Univ., Changwon, Gyeongnam, Korea

<sup>2</sup>Electrical Steel Research Team of Technical Research Lab., POSCO, Gyeongbuk, Korea  
jyecad@korea.com, lgh700@korea.com, jphong@sarim.changwon.ac.kr, khha@posco.co.kr

***Abstract*** – This paper deals with a design of a 2-phase Switched Reluctance(SR) Motor, which is used for a cooling fan motor of refrigerators. To reduce the dead zone and improve the efficiency, the snail-cam type rotor pole and the asymmetric stator pole are investigated. For the improved shape design, the performances of each model are obtained from numerical calculation results by 2D time-stepping finite element method (FEM) coupled with circuit equations. The accuracy of analysis is verified by comparing the analysis results with experimental data. Based on the investigation results, an improved shape of stator and rotor poles are proposed.

### Introduction

Switched Reluctance (SR) motors have many advantages, such as possibility of high-speed operation and simplicity of mechanical construction. These characteristics make SR motors be a good alternative to the other motors, such as Brushless DC and induction motors, and a better choice for the household electric appliances. Specially, the 2-phase SR motors have gained continuous attention of many researchers due to its low cost[1]-[2]. Even though the 2-phase SR motors can be attractive, it still has inherited disadvantages such as torque ripple and low efficiency in commercial applications. Therefore, in this paper the design of a 2phase SR motor is investigated to improve the torque characteristic and efficiency for the fan motor in refrigerators.

For the design of 2-phase SR motor as a part of electric appliance, there are several constraints. The number of stator and rotor poles, number of turns, and outer volume are fixed because the fan load, rated speed, and input voltage are constant and the system is compact. The shape of rotor and stator pole only can be changed for the design. Therefore the four design variables are selected, which are the stator pole arc, the ratio of the stator pole arc, the existence of the dip, and rotor slot depth. Analysis models are made by the combination of these variables, and for each analysis model the average torque and efficiency are calculated by using a hybrid method combining 2D finite element method (FEM) with the voltage equation.

2D solvers can be used effectively to estimate the magnetic characteristics of general lamination geometry, however it cannot be expected to give accurate magnetization curves for SR motors with short axial length because of the significant influence of end effects [1]. Furthermore the drive characteristic also should be considered since the switching states depending on drive are a great influence on phase current shapes. Therefore, the end effect is considered when inductance is calculated, and the dynamic simulation is accomplished with the consideration of the performance of drives. Finally, the accuracy of computation is verified by comparing the result with the experimental data of prototype motor.

As the results of the investigation, an improved asymmetric stator and snail-cam type rotor poles are proposed. Comparison of the torque characteristics of the prototype and the improved motor reveals that an asymmetric stator pole and a deeper slot depth of rotor eliminate dead zones, and result in higher efficiency.

## Analysis Model and Procedur

Fig. 1 shows the configuration of the prototype SRM as a cooling fan motor and its drive. This prototype motor has a wide dead zone and a low efficiency because it was designed in disregard of its switching state. The falling period of current is very short because of the switch-off voltage, which is over 5 times the switch-on voltage.

To solve the problems, firstly the converter was redesigned to asymmetric bridge converter. The drive is important to improve motor characteristics because longer falling period of current can improve the torque ripple, but it also can raise a reverse torque at the same time. Therefore the motor shapes are also changed in consideration of the converter. The motor variables are proposed as shown on Fig. 2. The redesign variables are stator pole arc, the ratio of stator pole arc, the existence of the dip and rotor slot depth as shown on right side of Fig. 2. The ratio of stator pole arc is the  $arc_1$  versus  $arc_2$ . The  $arc_1$  is longer side and the dip is on the other side,  $arc_2$ .

To improve the torque characters and efficiency, the variables are examined in 4 stages as follows:

1) Table 1 shows the initial combination of the variables. In this first stage, the switch turn-on angle is also considered because the switching angles influence current shape and magnetic characteristics of SRM. The base angle  $0^\circ$  is the position that stator and rotor poles are unaligned, and minus means the reverse direction to rotation. The big characters 'S' and 'A' mean symmetric and asymmetric pole shape, and the small characters 'a' and 'b' mean without and with dip, respectively. The number '10' and '20' is the absolute value of switch turn-on angle. Therefore, there are 8 type models in this stage.

2) In the second stage, the existence of dip and the stator pole arc are decided for 8 type models selected in the first stage. The range of the stator pole arc is from  $70^\circ$  to  $85^\circ$  as shown in Table 2. According to the general design equations in [1] and [2] the minimum stator pole arc is  $90^\circ$  in the case of 4-stator pole and 2-rotor pole SRM, but that is difficult to fabricate.

3) The ratio of stator pole arc is decided in the third stage. The ratio of symmetric stator pole is 1:1, and the ratios of asymmetric stator pole are the others as shown on Table 2. The switch turn-on angle is still considered in this stage.

4) After the decision of stator pole shape and switch turn-on angle in stage 3, the rotor slot depth is selected in the last stage. The range of rotor slot depth is from 2 to 8mm as shown on Table 2.

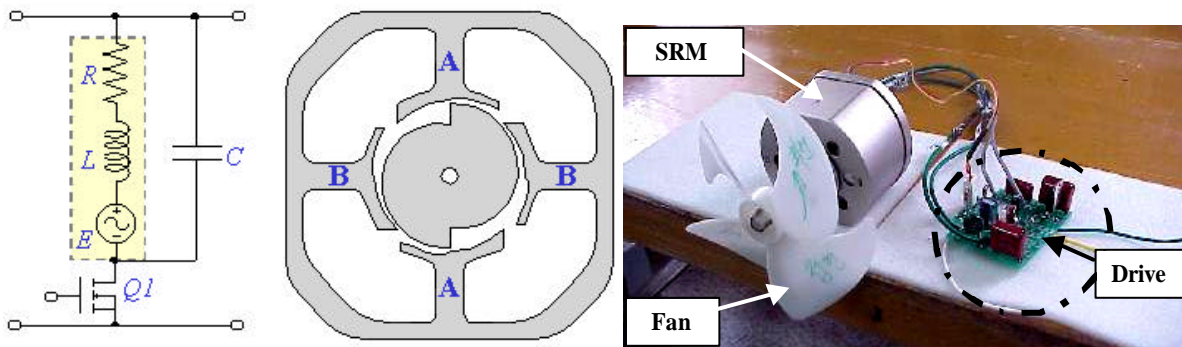


Fig. 1 The configuration of prototype drive and motor (left), and the picture (right)

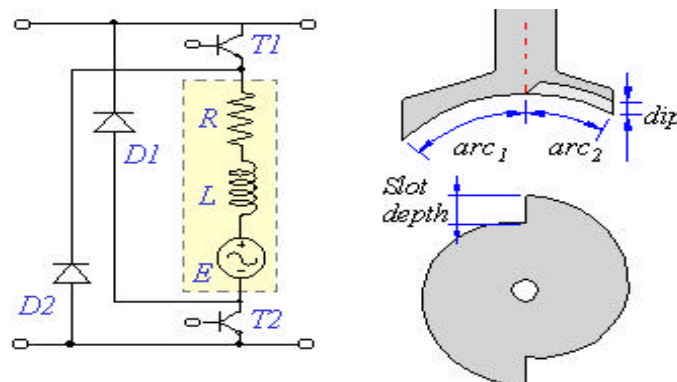


Fig. 2 Asymmetric bridge converter (left) and detail configuration of motor (right)

Table 1 Classification of Stator Pole Shapes

Switch Turn-on Angle (°)	Symmetric Pole (arc <sub>1</sub> : arc <sub>2</sub> = 1 : 1 )		Asymmetric Pole (arc <sub>1</sub> : arc <sub>2</sub> = 5 : 4 )	
	without dip	with dip	without dip	with dip
-10	S10a	S10b	A10a	A10b
-20	S20a	S20b	A20a	A20b

Table 2 Range of Variables

Stator Pole Arc (°)	70	75	80	85			
Ratio of Stator Pole Arc	1 : 1	9 : 8	5 : 4	3 : 2			
Rotor Slot Depth (mm)	2	3	4	5	6	7	8

Fig. 3 presents an analysis procedure by 2D FEM to select improved pole shapes. After combining the design variables, the linear inductance profiles are calculated at constant current condition to find the exact unaligned position. And then, the magnetic performances of the models selected in each stage as stated above are calculated from the nonlinear dynamic analysis at constant voltage condition. This process helps to evaluate the different structure models and therefore, stator and rotor pole shapes can be decided to improve the motor efficiency and eliminate the dead zone.

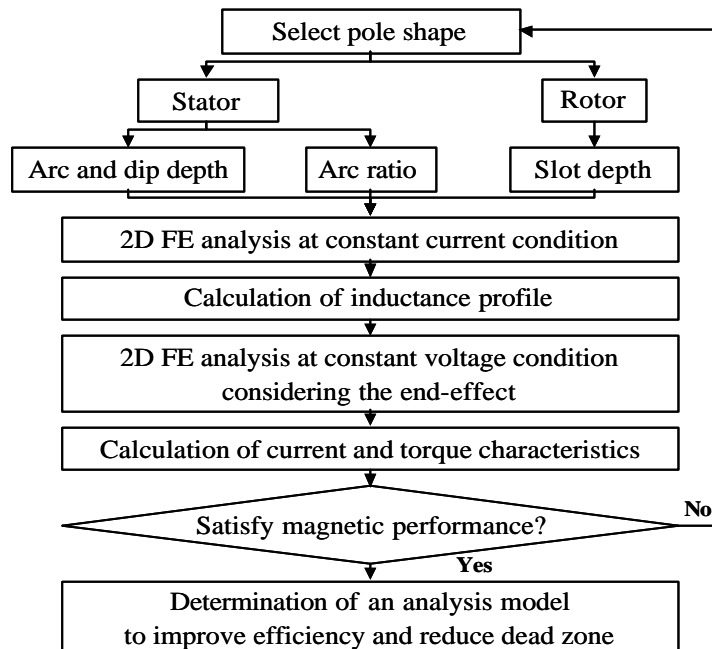


Fig. 3 Analysis procedure

## Analysis Method

### Electromagnetic Analysis

The electro-magnetic governing equation of SRM with field variable  $A$  is obtained by Maxwell's electromagnetic equation as follows:

$$\nabla \times \left( \frac{1}{\mu} \nabla \times A \right) = J_0 \quad (1)$$

where  $J_0$  is the applied current density,  $A$  is the magnetic vector potential and  $\mu$  is the magnetic permeability. For the analysis of the dynamic characteristics, voltage equation is coupled with (1) and then system matrix is obtained by time difference schemes. The method of the Maxwell stress tensor is used to calculate the static torque for the range of rotor position and phase excitation. Thus static torque is expressed according to the following (2).

$$\mathbf{T} = \oint_S \mathbf{r} \times \mathbf{P} \, dS \quad (2)$$

where  $\mathbf{r}$  is the distance vector of a point to axis rotation. Equation (2) is obtained by the surface integration of a stress tensor vector  $\mathbf{P}$  over an air gap enclosing the rotor surface  $S$ . The Maxwell stress tensor is given by (3)[3].

$$\mathbf{P} = \frac{1}{\mu_0} (\mathbf{n} \otimes \mathbf{B}) \mathbf{B} - \frac{1}{2\mu_0} B^2 \mathbf{n} \quad (3)$$

where  $\mu_0$  is the permeability of free space,  $\mathbf{n}$  is the normal vector to the surface  $S$ ,  $\mathbf{B}$  is the magnetic flux density.

### End Effect Calculation

From the electromagnetic analysis by 2D FEM, the linkage flux is calculated by difference between vector potentials at the both sides of an excited coil. Inductance is obtained by the ratio of the linkage flux and exciting current [4], but the results are not accurate because the consideration of axial fringing effect is impossible in 2D FEM. For considering the end coil effect, empirical formulations should be developed by the equations in [5], [6] and [7]. In this paper, the end effect for the unaligned and aligned inductance is calculated by the equation in [7].

## Design and Analysis Results

### Analysis and Measurement of ProTOTYPE

The comparison of measured and calculated inductance for prototype motor is shown in Table 3. The error between the two inductances is under 5%. Fig. 4 shows the currents and torque of the machine. The current is obtained by experiment, and these results are compared with those of the analysis by FEM. Since the currents aspects coincide, the torque can be expected as shown in the lower part of Fig. 4. The efficiency of this motor is about 52.6%, but the dead zone is 16%.

### Inductance Profiles of analysis models

Fig. 5 shows the linear inductances of each analysis model, which consists of the variables on Table 2 and 1. In this figure, the rotor positions are not absolute, and the start point (0°) is where the inductance is the minimum. The profiles are different from each other with respect to stator pole arc and the existence of dip. But because the saturation is neglected in the magnetic materials, the inductance profiles are same for the symmetric and asymmetric pole shapes, and the inductance of symmetric stator pole are only shown in Fig. 5. The wider pole arc makes the longer increase span and the dip makes the sharp drop in the decrease span.

### Stator and Rotor Pole Design

Fig. 6 shows the comparison of the effective minimum torque (EMT) and the efficiency of the models on Table 1 with respect to the stator pole arc on Table 2. The EMT is the ratio of minimum torque to average torque. When this value is greater than zero, there is no dead zone, and the relative magnitude makes comparison of torque ripple of each model possible. In the most cases, the existence of dip and smaller stator pole arc makes higher EMT and lower efficiency. Fig. 7 shows the results of analysis for the ratio of stator pole arc when the stator pole arc is 80° without dip. The EMT and the efficiency depend on the ratio of the stator pole and the switch turn-on angle. The highest efficiency is obtained when the ratio is 5:4 and switch turn-on angle is -10°. The EMT of this pole shape is also greater than zero. After the decision of stator pole shape and switch turn-on angle, the rotor slot depth

is selected for the last stage. Fig. 8 shows the average torque, the EMT and the efficiency with rotor slot depth. All performances increase until the rotor slot depth is 6mm. From the above investigation, the SRM for the cooling fan is redesigned. The configuration and the performances are numerically compared with the prototype on Table 4. The efficiency is increased by 2.1% and dead zone is eliminated. The torque profile of redesigned motors is on Fig. 4 and this is graphically compared with that of prototype.

Table 3 Comparison of measured and calculated inductances of prototype

	Measured Inductance (mH)	Calculated Inductance (mH)			Error (%)
		2D FEM	End Effect	Sum	
Aligned	173.18	169.07	12.41	181.48	4.79
Unaligned	79.78	50.86	27.01	77.87	2.39

Table 4 Comparison of prototype and improved model

	Prototype	Improved Model
Stator Pole Arc (°)	85	80
Ratio of Stator Pole Arc	9 : 8	5 : 4
Existence of Dip	Yes	No
Rotor Slot Depth (mm)	4	6
Average Torque (kgf-cm)	79.6	83.0
Efficiency (%)	52.6	54.7
Dead Zone (°)	16	0

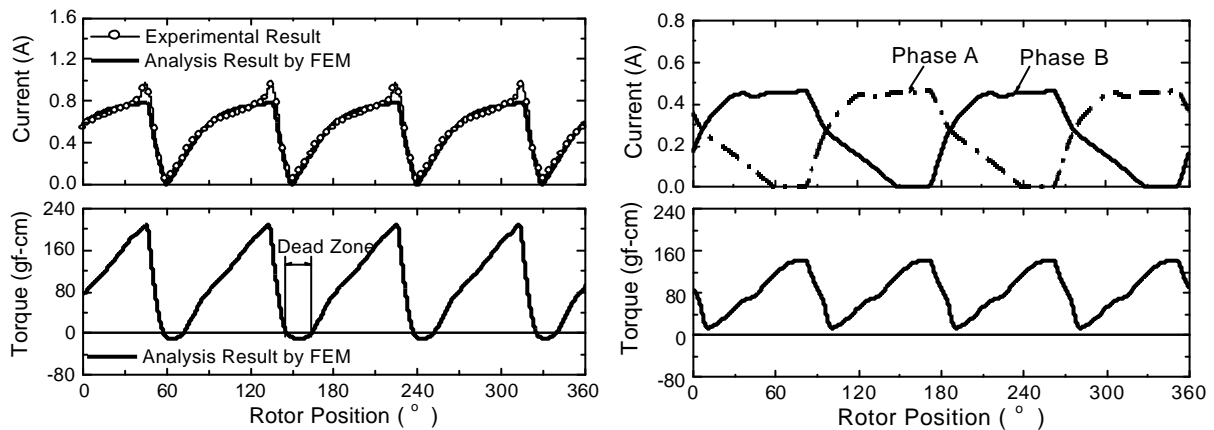
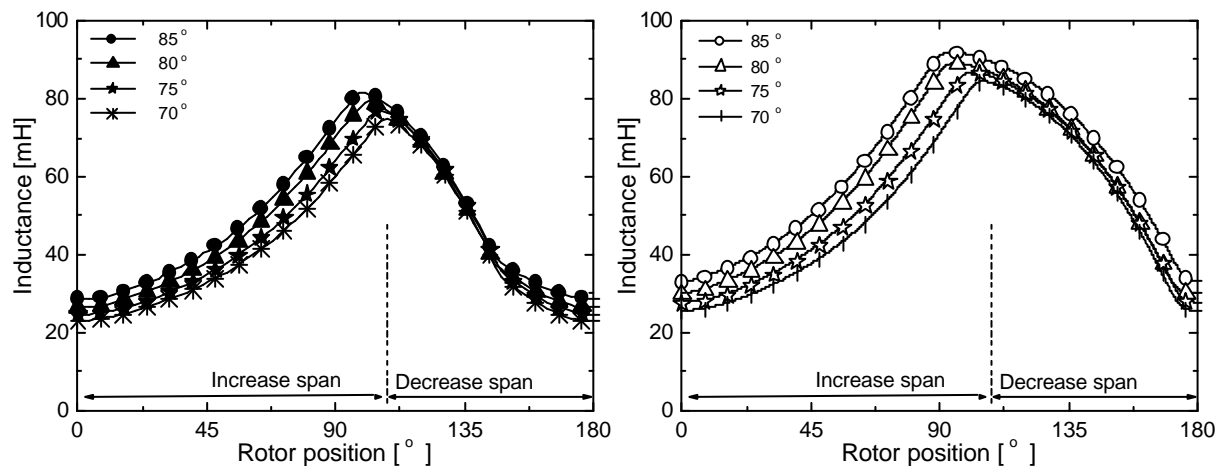


Fig. 4 Current and torque of prototype (left) and improved model (right)



(a) Symmetric stator pole with dip

(b) Symmetric stator pole without dip

Fig. 5 Inductance profiles for rotor position and stator pole arc

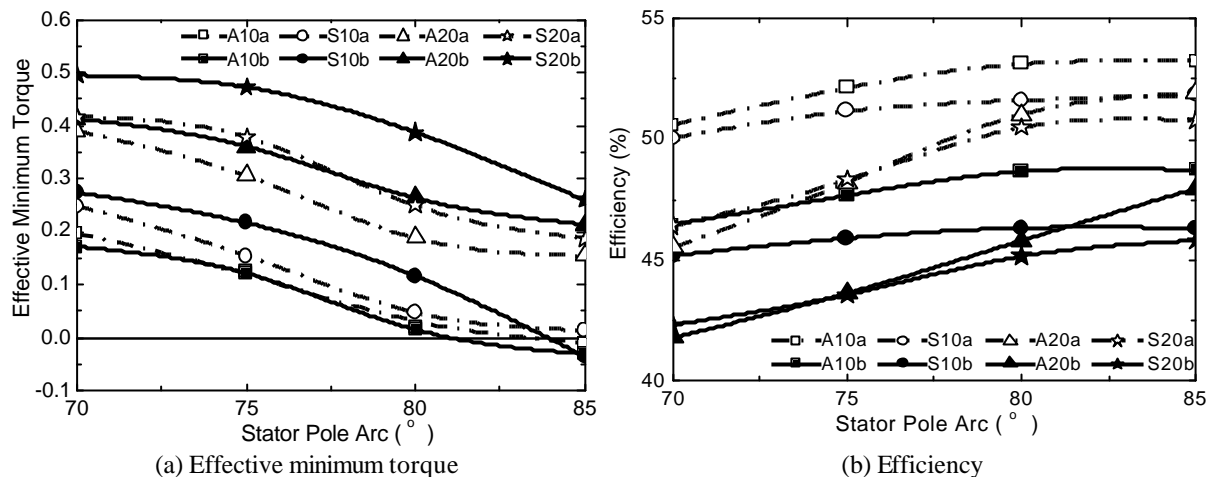


Fig. 6 Effective minimum torque and efficiency with respect to stator pole arc

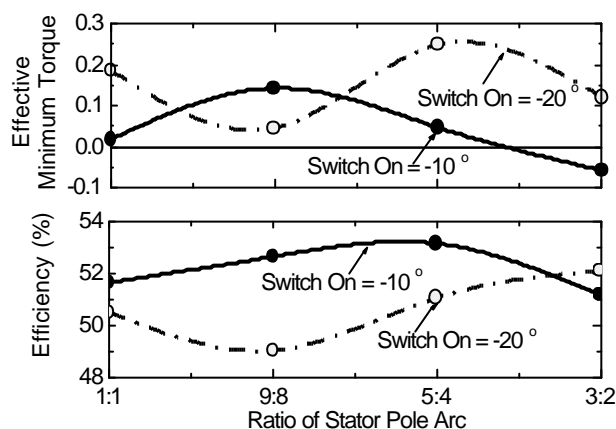


Fig. 7 Effective minimum torque and efficiency with respect to the ratio of stator pole arc

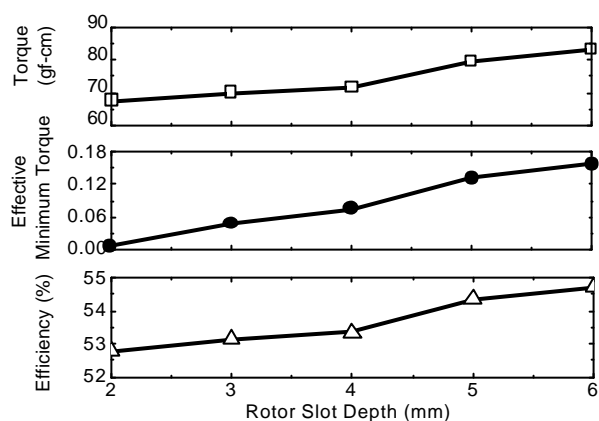


Fig. 8. Average torque, effective minimum torque and efficiency with respect to the rotor slot depth

## Conclusions

This paper demonstrates the effect of stator and rotor pole shapes on torque characteristics for 2-phase SRM. The detail trends of the performance according to the various design parameters are investigated by 2D time stepping FEM coupled with voltage equations. From the redesigned results, the improved motor has an asymmetric stator pole and a snail-cam rotor with deeper slot depth. The efficiency of the redesigned motor is higher than the original prototype and the dead zone is completely eliminated.

## REFERENCES

- [1] T. J. E. Miller, *Switched Reluctance Motors and Their Control*, Magna physics publishing and Clarendon Press Oxford, 1993.
- [2] P. J. Lawrenson and el. "Variable-speed switched reluctance motors," *IEE Proceeding*, Vol. 127, pp. 253-265, July, 1980
- [3] M. J. DeBortoli and S. J. Salon, "Computation of forces and torque in electromagnetic devices using the finite element method," *International Conference on Electrical Machines*, pp. 699-705, August, 1990
- [4] Koichi Koibuchi and el, "A Basic Study for Optimal Design of Switched Reluctance Motor by Finite Element Method," *IEEE Trans. on Magnetics*, Vol. 33, pp. 2077-2080, March, 1997
- [5] J. Corda and J. M. Stephenson, "Analytical estimation of the minimum and maximum inductances of a double-salient motor," in *Proceedings of the International Conference on Stepping Motors and Systems*, Lees, U. K., pp.50-59, September, 1979
- [6] Yifan Tang, "Characterization, Numerical Analysis, and Design of Switched Reluctance Motors," *IEEE Trans. on Industry Application*, Vol. 33, pp. 1544-1552, November/December, 1997.
- [7] User's Manual of PC-SRD VERSION 7.0, SPEED CONSORTIUM, 1999



XI INTERNATIONAL SYMPOSIUM  
ON **ELECTROMAGNETIC FIELDS**  
IN ELECTRICAL ENGINEERING  
**ISEF 2003**



SEPTEMBER 18-20, 2003

MARIBOR, SLOVENIA

**The Symposium is organised by:**

- Research group Applied Electromagnetics, Faculty of Electrical Engineering and Computer Science, Maribor, Slovenia
- University of Maribor, Slovenia
- Institute of Mechatronics and Information Systems, Technical University of Lodz, Poland
- Department of Fundamental Research, Electrotechnical Institute, Warsaw, Poland

VOLUME 1

7. <b>The Influence of Brush Shift on EMF in Small Commutator Machines</b> M. Klauz, T.JE Miller .....	777
8. <b>An Improved 2-Phase Snail-Cam Type Fan Motor Design</b> J.Y. Lee, G.H. Lee, J.J. Lee, J.P. Hong, K.H. Ha .....	783
9. <b>Design and Characteristic Analysis of Skeleton Type Single-Phase Brushless DC Motor Using Finite Element Method</b> Y.S. Lim, K.H. Ha, J.J. Lee, J.P. Hong.....	789
10. <b>Analysis of Magnetization Characteristics of HTS Bulk Rotor in a Rotating Magnetic Field</b> T. Nakamura, H.J. Jung, N. Tanaka, I. Muta, K. Fukui .....	795
11. <b>The 3D Dynamic Simulation of the Inverter Fed Electromechanical Actuators Including Eddy Currents</b> L. Nowak.....	801
12. <b>Analysis and Design Program of Switched Reluctance Motor Using an Analytical Method</b> P.J. Otaduy, J. McKeever, D. Adams, P.S. Shin.....	805
13. <b>Influence of Machine Symmetry on Cogging Torque in Variable Reluctance Permanent-Magnet Motors</b> H. Öztura .....	811
14. <b>Power Losses Analysis in the Windings of Electromagnetic Gear</b> A. Patecki, S. Stępień, G. Szymański.....	817
15. <b>Evaluation of New Surface Mounted Permanent Magnet Synchronous Machine with Finite Element Calculations</b> T. Schneider, A. Binder.....	823
16. <b>Parameterization Coupling Model of Saturated Linear Synchronous Reluctance Motor and Its Parameters</b> G. Štumberger, B. Štumberger, D. Dolinar.....	829
17. <b>Finite Element Analysis of the Magnetorheological Fluid Brake Transients</b> W. Szeląg .....	835
18. <b>Analysis of Supplementary Conditions for a Smooth Torque Running of Heteropolar Excited Vernier Reluctance Machines</b> S. Taïbi, Th. Henneron, A. Tounzi.....	841
19. <b>Numerical Analysis of the Brushless Motor Magnetic Field and Torque</b> I. Tičar, A. Stermecki, I. Zagradišnik.....	847
20. <b>3-D FEA and Topology Optimization of Linear Motor for Linear Compressor</b> S. Wang, J. Kang, H. Lee, E. Hong, K. Park .....	853
21. <b>Effect of Coil Shapes on Thrust Characteristics of Linear Induction Motor</b> T. Yamaguchi, Y. Kawase, T. Eguchi.....	859
22. <b>Frequency Discriminator Based on Dielectric Resonator and Hybrid Ring</b> E.Y. Yuksel, T.T.Y. Wong.....	863